Molecular Pharmacology Fast Forward. Published on July 8, 2011 as doi:10.1124/mol.111.073809
This article has not been copyedited and formatted. The final version may differ from this version.

MOL #73809

Molecular determinants for activation of human ERG1 potassium channels by 3-nitro-N-(4-phenoxyphenyl) benzamide

Vivek Garg, Anna Stary-Weinzinger, Frank Sachse and Michael C. Sanguinetti

Department of Physiology (V.G., M.C.S.), Nora Eccles Harrison Cardiovascular Research & Training Institute (V.G., F.S., M.C.S.), and Department of Bioengineering (F.S.), University of Utah, Salt Lake City, Utah ; Department of Pharmacology and Toxicology, University of Vienna, Vienna, Austria (A.S.-W.)

Molecular Pharmacology Fast Forward. Published on July 8, 2011 as DOI: 10.1124/mol.111.073809
This article has not been copyedited and formatted. The final version may differ from this version.

Running Title Page

Running title: hERG1 channel activator

Corresponding author:
Michael C. Sanguinetti, PhD
Nora Eccles Harrison Cardiovascular Research and Training Institute
Department of Physiology
University of Utah
95 South 2000 East
Salt Lake City, Utah 84112
Tele: 801-581-3058
Fax: 801-581-3128
Email: sanguinetti@cvrti.utah.edu

#of text pages: 28

# of figures: 6

# of references: 47

# of words in the *Abstract*: 211

# of words in the *Introduction*: 526

# of words in the *Discussion*: 955

Supporting Information: 5 Supplemental Figures

ABBREVIATIONS: hERG1, human *ether-a-go-go*-related gene 1; I_{test}, current activated by membrane depolarization; I_{tail}, tail current; I-V, current-voltage; LQTS, long QT syndrome; ICA, 3-nitro-N-(4-phenoxyphenyl) benzamide; V_t, test potential; $V_{0.5}$, half-point of Boltzmann relationship; WT, wild-type

Molecular Pharmacology Fast Forward. Published on July 8, 2011 as DOI: 10.1124/mol.111.073809
This article has not been copyedited and formatted. The final version may differ from this version.

Abstract

Human *ether-a-go-go-related* gene 1 (hERG1) channels mediate repolarization of cardiac action potentials. Inherited long QT syndrome (LQTS) caused by loss-of-function mutations, or unintended blockade of hERG1 channels by many drugs, can lead to severe arrhythmia and sudden death. Drugs that activate hERG1 are a novel pharmacological approach to treat LQTS. Recently, ICA-105574 (3-nitro-N-(4-phenoxyphenyl) benzamide, ICA) was discovered to activate hERG1 by strong attenuation of P-type inactivation. Here we utilized scanning mutagenesis of hERG1 to identify the molecular determinants of ICA action. Three mutations abolished the activator effects of 30 μM ICA, including L622C in the pore helix, F557L in the S5 segment and Y652A in the S6 segment. One mutation in S6 (A653M) switched the activity of ICA from an activator to an inhibitor, revealing its partial agonist activity. This was confirmed by showing that the non-inactivating mutant hERG1 channel (G628C/S631C) was inhibited by ICA and that addition of the F557L mutation rendered the channel drug-insensitive. Simulated molecular docking of ICA to homology models of hERG1 corroborated the scanning mutagenesis findings. Together our findings indicate that ICA is a mixed agonist of hERG1 channels. Activation or inhibition of currents is mediated by the same or overlapping binding site located in the pore module between two adjacent subunits of the homotetrameric channel.

Molecular Pharmacology Fast Forward. Published on July 8, 2011 as DOI: 10.1124/mol.111.073809
This article has not been copyedited and formatted. The final version may differ from this version.

Introduction

The rapid delayed rectifier K^+ current (I_{Kr}) conducted by human *ether-a-go-go-related* gene 1 (hERG1) channels is the predominant repolarizing current of cardiac action potentials in large mammals (Sanguinetti et al., 1995; Trudeau et al., 1995). Slow activation/deactivation and rapid inactivation of hERG1 channels leads to a peak in I_{Kr} during phase 3 repolarization and thus is a critical regulator of action potential duration and heart rate (Sanguinetti and Tristani-Firouzi, 2006). Inherited loss-of-function mutations in hERG1 can induce torsades de pointes (TdP) ventricular arrhythmia (Curran et al., 1995) and accounts for ~40% of all cases of congenital long QT syndromes (LQTS). A gain-of-function mutation in hERG1 has been associated with the rare short-QT syndrome (Brugada et al., 2004). Prolonged QT duration and TdP is most commonly an acquired disorder, often caused by block of hERG1 channels as a toxic side effect of several commonly used medications (Sanguinetti and Tristani-Firouzi, 2006). Individuals with either inherited or acquired LQTS are at an increased risk of cardiac arrhythmia and sudden death.

Congenital LQTS is commonly treated by administration of a β-adrenergic receptor blocker, and invasive and costly implantable defibrillators are used for the most severe cases. The available options for acute drug-induced TdP are intravenous Mg^{2+}, correction of any electrolyte disturbance, and discontinuation of the culprit drug. These options are inadequate for many patients and a mechanistic-based approach such as enhancing the cardiac repolarizing currents I_{Kr} or I_{Ks} has been proposed (Goldenberg and Moss, 2008). Recently several compounds that activate hERG1 channels were fortuitously discovered during routine off-target screening for channel block (Gerlach et al., 2010; Hansen et al., 2006; Kang et al., 2005; Zhou et al., 2005). The mechanisms of action of hERG1 activators include suppression of pore (P)-type inactivation and slowed deactivation. The putative binding site for two hERG1 activators, RPR260243 (Kang et al., 2005) and PD-118057 (Zhou et al., 2005) were recently described. The binding sites are distinct and can intuitively explain the predominant mechanism of action of each specific activator. RPR260243 binds near the intracellular gate of the channel (and close to S4-S5 linker)

Molecular Pharmacology Fast Forward. Published on July 8, 2011 as DOI: 10.1124/mol.111.073809
This article has not been copyedited and formatted. The final version may differ from this version.

and markedly slows deactivation while also affecting inactivation by an undefined allosteric mechanism (Perry et al., 2007). PD-118057 binds to a pocket formed by the pore helix of one subunit and nearby S6 residues of an adjacent subunit to modestly attenuate P-type inactivation and increase single channel open probability (P_o) with only minor effects on deactivation (Perry et al., 2009).

Recently, another activator of hERG1, ICA-105574 (3-nitro-N-(4-phenoxyphenyl) benzamide) was reported to shorten action potential duration of isolated guinea pig cardiomyocytes in a concentration-dependent manner (Gerlach et al., 2010). At the maximally effective concentration, ICA induced a +180 mV shift in the voltage half-point ($V_{0.5}$) of inactivation, resulting in an increased outward current of 10-15 times the basal amplitude at 0 mV and slowed the rate of hERG1 current deactivation by 2-fold (Gerlach et al., 2010). To elucidate the molecular determinants for the effects of ICA, we used scanning mutagenesis of the pore region of hERG1, expression of mutant channels in *Xenopus* oocytes and voltage clamp for functional analysis of mutant channels and determined the effects of ICA on inactivation-impaired hERG1 mutant channels.

Molecular Pharmacology Fast Forward. Published on July 8, 2011 as DOI: 10.1124/mol.111.073809
This article has not been copyedited and formatted. The final version may differ from this version.

Materials and Methods

Channel Mutagenesis and Expression in *Xenopus* Oocytes. *HERG1* (*KCNH2*, isoform 1a), was cloned into the pSP64 oocyte expression vector, and mutations were introduced using the QuikChange mutagenesis kit (Agilent Technologies, CA). Residues L553-I567 in S5, T618-S624 in PH and C643-I663 in S6 were mutated to Ala or Cys (to Gly or Val for Ala residues). For some residues, alternate substitutions were introduced to enhance expression (F557L, L622C, F656T and A661C). Amino acid substitutions at some residues expressed poorly (H562, W568, and I655) and were not studied further. cRNA was prepared by in vitro transcription with mMessage mMachine SP6 kit (Ambion, Austin, TX) after linearization of the vector plasmid with Eco*R1*. The isolation, culture, and injection of oocytes with cRNA were performed as previously described (Goldin, 1991; Stuhmer, 1992).

Voltage Clamp. Whole cell hERG1 currents were recorded from oocytes 1 to 4 days after cRNA injection by using the two-microelectrode voltage clamp technique (Stuhmer, 1992). Agarose-tipped microelectrodes (Schreibmayer et al., 1994) were fabricated by filling the tips of 1 mm O.D. borosilicate pipettes with 1% agarose dissolved in 3 M KCl and then back-filling with 3 M KCl. Oocytes were voltage clamped to a holding potential of −100 mV, and 1-s pulses to a test potential (Vt) of 0 mV were applied every 15 s until current magnitude reached a steady-state level. For standard *I-V* relationship, step currents were elicited with 1-s pulses from −100 to +50 mV in 10 mV increments. Tail currents were measured at −70 mV. For highly inactivated mutant channels, currents were recorded from oocytes bathed in a Na^+-free extracellular solution with $[K^+]_e$ elevated to 104 mM. Step currents were elicited with 1-s pulses to a Vt that ranged from −100 to +40 mV in 10 mV increments. After each test pulse, the membrane was repolarized to −120 mV. Peak tail currents were plotted as a function of Vt measured before and after 30 μM ICA-105574 (ICA). Values were normalized to the peak values of the control currents (at +40 mV) and the data were fitted to a Boltzmann function to determine the half-point of activation

Molecular Pharmacology Fast Forward. Published on July 8, 2011 as DOI: 10.1124/mol.111.073809
This article has not been copyedited and formatted. The final version may differ from this version.

($V_{0.5}$) and the slope factor (k) of the relationship. Other voltage pulse protocols are described under *Results* and in the figure legends.

After addition of ICA to the bathing solution, 1-s pulses to 0 mV were applied every 30 s until a new steady-state level was achieved or until 10 min. Relevant voltage protocols were then repeated in the presence of drug.

Gating currents of non-conducting G626A hERG1 mutant channels were measured using the cut-open oocyte Vaseline gap (COVG) method (Bezanilla and Stefani, 1998), with pulse protocols and solutions optimized for characterizing hERG1 gating currents (Piper et al., 2003). The external solution in the top and guard chambers contained (in mM): 120 tetraethylammonium 4-morpholine ethanesulfonic acid (TEA-MES), 2 Ca-MES, 10 HEPES, (pH 7.4 with MES). The internal solution in the bottom compartment contained (in mM): 120 K-MES, 2 EDTA, 10 HEPES, (pH 7.4 with MES). Signals were low-pass filtered at 10 kHz and digitized at 40 kHz. Linear leak and capacitance currents were compensated by analog circuitry and subtracted online by using a p/−8 protocol.

Single hERG1 channel currents were measured in cell-attached patches as described previously (Zou et al., 1997) using standard techniques (Hamill et al., 1981) and an Axopatch 200B amplifier (Molecular Devices, Sunnyvale, CA). Electrode resistance was 8-12 MΩ when pipettes were filled with a solution containing (in mM): 104 K-gluconate, 2 $MgCl_2$, 10 HEPES, pH 7.2 with KOH. The bath solution contained (in mM): 140 KCl, 0.1 $CaCl_2$, 2 $MgCl_2$, 10 HEPES, pH 7.2 with KOH. Single channel current amplitudes were determined from analysis of all points amplitude histograms (pCLAMP 9) of currents filtered at 1 kHz and digitized at 5 kHz. Data are expressed as mean ± standard error (*n* = number of oocytes) and analyzed by the Student's t-test.

Molecular Modeling. The homology model of the closed channel conformation was generated with Modeller9v7 using the KcsA crystal structure (pdb ID: 2HVK) as template.

Molecular Pharmacology Fast Forward. Published on July 8, 2011 as DOI: 10.1124/mol.111.073809
This article has not been copyedited and formatted. The final version may differ from this version.

Modeling details, including coordinates for the open conformation have been described previously (Stary et al., 2010).

Mutants F557L, L622C, Y652A and A653M of hERG1 were generated in Pymol. MD simulations of closed models were performed with Gromacs v.4.5.4 (Hess et al., 2008). WT and mutant channels were embedded in an equilibrated simulation box of palmitoyloleoyl phosphatidylcholine (POPC) lipids. Lipid parameters were taken from Berger et al. (Berger et al., 1997), and the OPLS-all-atom force field (Jorgensen et al., 1996) was used for the protein. The solvent was described by the TIP4P water model (Jorgensen et al., 1983). Electrostatic interactions were calculated explicitly at a distance <1 nm, long-range electrostatic interactions were calculated at every step by particle-mesh Ewald summation (Darden et al., 1993). Lennard–Jones interactions were calculated with a cutoff of 1 nm. All bonds were constrained by using the LINCS algorithm (Hess et al., 1997), allowing for an integration time step of 2 fs. The Nose-Hoover thermostat (Nose, 1984) was used for temperature coupling (τ = 0.1 ps) and the Parrinello-Rahman barostat algorithm (Parrinello and Rahman, 1981) for pressure coupling. 1000 conjugate gradient energy-minimization steps were performed, followed by 2 ns of restrained MD in which the protein atoms were restrained with a force constant of 1000kJ/mol^{-1}nm^{-2} to their initial position, while ions, lipids and solvent were allowed to move freely. Each system was then subjected to 2 x 10 ns of unrestrained MD, during which coordinates were saved every 1 ps for analysis.

Coordinates of ICA105574 were generated with Gaussview 5 and the geometry optimized with the Hartee-Fock 3-21G basis set implemented in Gaussian09 (Frisch et al., 2009). Docking was performed with the program Gold 4.0.1 (Jones et al., 1995). Coordinates of the geometric center calculated among residues F557, L622, Y652 and A653 were taken as binding site origin. The binding site radius was set equal to 10 Å. 150,000 operations of the GOLD genetic algorithm were used to dock the selected compounds into the WT and mutant channels. 3 snapshots (3 ns, 6 ns, 8 ns) were taken from MD trajectories. The Chemscore scoring function

Molecular Pharmacology Fast Forward. Published on July 8, 2011 as DOI: 10.1124/mol.111.073809
This article has not been copyedited and formatted. The final version may differ from this version.

was used to estimate free energies of binding (Gold.Chemscore.DG). Reported values are averaged over the 10 best docking poses.

Solutions and Drugs. For two-microelectrode voltage clamp experiments, the extracellular solution contained the following (in mM): 98 NaCl, 2 KCl, 1 $CaCl_2$, 1 $MgCl_2$, 5 HEPES (pH 7.6). ICA was purchased from Sigma-Aldrich (St. Louis, MO; catalog #R595047). Drug solutions were prepared fresh just before experiment by dilution of a 10 mM DMSO stock solution of ICA. Each oocyte was treated with a single concentration (30 μM) of drug unless specified otherwise.

Results

ICA increases hERG1 current by suppressing inactivation but has no effect on single channel conductance, maximal conductance or gating currents. The effects of 10 and 30 μM ICA on wild-type (WT) hERG1 channels expressed in *Xenopus* oocytes are illustrated in Fig. 1A and B. ICA induced a marked concentration-dependent enhancement of current magnitude. Activation of hERG1 current by 30 μM ICA reached a steady-state in ~10 min at 30 μM. The fold-increase in current assayed with 1 s pulses to a test potential (Vt) of +20 mV was 7.6 ± 1.1 at 10 μM and 28 ± 3.4 at 30 μM, (n = 3 - 8). The potency of ICA was reduced in oocytes compared to that reported (Gerlach et al., 2010) for HEK293 cells (EC_{50} = 0.5 μM), probably because ICA is highly lipophilic (logP = 3.69) and accumulates in the yolk of oocytes (Witchel et al., 2002). The increase in current by ICA was associated with a marked decrease in rectification of the current-voltage (I-Vt) relationship (Fig. 1B) and an enhanced effect at more positive test potentials (Fig. 1C), effects consistent with a large drug-induced positive shift in the $V_{0.5}$ of inactivation as reported previously (Gerlach et al., 2010). ICA binds to the closed state of the hERG1 channel (Gerlach et al., 2010). In Fig. 1D we show that ICA can also bind to channels

Molecular Pharmacology Fast Forward. Published on July 8, 2011 as DOI: 10.1124/mol.111.073809
This article has not been copyedited and formatted. The final version may differ from this version.

when applied to an oocyte during a prolonged depolarizing step to +30 mV, indicating that the drug can also bind to channels in the open or inactivated state.

The voltage dependence of the hERG1 channel conductance-voltage (G-V) relationship was determined by measuring peak tail currents (I_{tails}) after a 1-s depolarizing pulse to a variable Vt. For these experiments, oocytes were bathed in 20 mM $[K^+]_o$ solution to preclude variation in I_{tail} magnitude caused by the transient local accumulation of extracellular K^+ and thus, chemical driving force associated with large outward currents and low $[K^+]_o$. When I_{tails} were elicited at −140 mV, a potential where recovery from inactivation is rapid and complete, ICA did not alter the voltage dependence or G_{max} of the G-V relationship for hERG1 (Fig. 1E). This finding suggests that ICA does not cause any significant change in single channel activity or induce recruitment of channels to the surface membrane. To confirm these expectations, we determined the effect of ICA on single channel conductance and gating currents.

Single hERG1 channel activity was determined in cell-attached patches of oocytes using pipettes filled with 104 mM $[K^+]_o$ solution (Supplemental Fig. 1). The slope conductance for single channel activity was not altered when 30 μM ICA was included in the pipette and bath solution (Fig. 1F). Although unlikely, ICA might also increase current magnitude by recruiting channels from a cytoplasmic store to the plasma membrane. As an indirect measure of plasma-membrane bound channel density, we determined the maximum intramembrane charge displacement ($Q_{OFF\text{-}max}$) associated with the OFF gating current. The cut-open oocyte voltage clamp technique (Stefani and Bezanilla, 1998) was used to measure hERG1 gating currents. ICA had no effect on the kinetics of gating currents or the magnitude of the maximum intramembrane charge displacement ($Q_{OFF\text{-}max}$) associated with the OFF gating current when compared to currents treated with vehicle (DMSO) (Fig. 1G and Supplemental Fig. 1). Together these findings indicate that the ICA-induced increase in hERG1 current is not due to an increase in maximum whole cell conductance, single channel conductance, or an increased number of functional channels at the

Molecular Pharmacology Fast Forward. Published on July 8, 2011 as DOI: 10.1124/mol.111.073809
This article has not been copyedited and formatted. The final version may differ from this version.

surface membrane and thus, can be attributed solely to a marked attenuation of P-type inactivation (Gerlach et al., 2010).

To further explore the role of inactivation in the mechanism of action of ICA, its effects on three inactivation-impaired mutant hERG1 channels were determined (Fig. 2). S620T hERG1 channels have greatly reduced inactivation (Ficker et al., 1998) and as expected, exhibited a greatly reduced response to ICA (only 1.3 ± 0.2 fold increase at +50 mV, n = 7). Two other point mutations (S631A, N588K) also attenuate hERG1 inactivation (Brugada et al., 2004; Schonherr and Heinemann, 1996), albeit to a lesser extent than the S620T mutation and as expected, these channels were more sensitive to the drug compared to S620T hERG1 channels (Fig. 2). At +50 mV, 30 μM ICA increased S631A channel currents by 3.2 ± 0.2 fold (n = 4) and N588K channel currents by 2.4 ± 0.1 fold (n = 3), far less that the 47-fold enhancement observed for WT hERG1 channels (Fig. 1C). Thus, current enhancement by ICA is strongly correlated with the extent of intrinsic P-type inactivation of hERG1 channels.

Molecular determinants for ICA binding. Based on mutational analysis of hERG1 (Ficker et al., 1998), the entire pore module, including the pore helix/selectivity filter (PH/SF), S5 and S6 segments participate in channel inactivation. To determine the molecular determinants of ICA activity, we performed scanning mutagenesis of major portions of the hERG1 pore module (Fig. 2A). A total of 44 residues were mutated, including L553-I567 in S5, T618-S624 in the PH/SF and C643-I663 in S6. The effect of ICA (30 μM for 10 min) on individual mutant channels was quantified as the fold-increase in outward current measured at the end of a 1-s pulse to a Vt of +20 mV (Fig. 2B).

Nine mutations attenuated the response to 30 μM ICA by ≥10-fold and were classified as 'high impact' residues (Fig. 2B). All of these mutant channels exhibited normal P-type inactivation as revealed by their typical bell-shaped I-Vt relationships. Three mutations prevented the activation of hERG1 by ICA. F557L and L622C channels were completely insensitive to 30 μM ICA (Fig. 4A, B). ICA induced a slight, but insignificant increase in outward Y652A channel

Molecular Pharmacology Fast Forward. Published on July 8, 2011 as DOI: 10.1124/mol.111.073809
This article has not been copyedited and formatted. The final version may differ from this version.

currents and accelerated the rate of current deactivation; at −70 mV, the time constants for fast and slow phases of deactivation (τ_f and τ_s) were 99 ± 9.8 ms and 329 ± 36 ms for control, as compared to 53 ± 8.3 ms and 221 ± 37 ms for 30 μM ICA (n = 6). Currents at +20 mV for five other mutant channels (F619A, S624A, F656T, N658A, V659A) were increased <3-fold by 30 μM ICA (Supplemental Fig. 2). ICA inhibited one mutant hERG1 channel (A653M) and accelerated its rate of deactivation (Fig. 4D); at −70 mV, τ_f and τ_s were 60 ± 3.9 ms and 283 ± 25 ms for control, as compared to 41 ± 3.7 and 216 ± 27 ms for drug (n = 6). In contrast to Y652A and A653M channels, ICA slowed the rate of monoexponential deactivation of WT channels at −70 mV by ~2-fold, from 413 ± 10 ms to 751 ± 62 ms (n = 6). Four mutant channels (T618A, T623A, M645C and G648A) exhibited enhanced inactivation or very low expression and were therefore recorded in an extracellular solution containing 104 mM K^+ to accentuate the magnitude of inward I_{tail}. ICA enhanced T618A channel currents, but reduced T623A, M645C and G648A channel currents by 30–50% (Supplemental Fig. 3). In summary, scanning mutagenesis identified three mutations (F557L, L622C, Y652A) that eliminated or attenuated the activator effects as well as four mutations (T623A, M645C, G648A, A653M) that revealed an inhibitory activity of ICA.

F557, L622 and Y652 are likely key components of the binding site for ICA since both activator and inhibitory effects were prevented by mutation of these residues. T623, S624, M645, G648, Y652, F656 and V659 line the internal cavity and some of these residues are important molecular determinants for pore block by hERG1 channel inhibitors (Mitcheson et al., 2000). Several of the high impact residues identified here for ICA were previously found to be important for other hERG1 activators, including RPR260243 (F557, Y652, N658 and V659) (Perry et al., 2007) and PD-118057 (F619, L622, M645) (Perry et al., 2009). Thus, the molecular determinants of channel activation by ICA overlap, but are not identical to, other well characterized hERG1 activators and blockers.

Molecular Pharmacology Fast Forward. Published on July 8, 2011 as DOI: 10.1124/mol.111.073809
This article has not been copyedited and formatted. The final version may differ from this version.

Simulated docking of ICA on hERG1. A homology model of the hERG1 pore module was constructed by using the KcsA (closed state) and KvAP (open state) channel structures as templates. ICA binds perpendicular to the channel axis between two adjacent subunits of the pore module in both the open (Fig. 5A) and closed (Fig. 5C) state. A close-up view of the putative drug-binding region is depicted in Fig. 5B and 5D where the high impact residues identified by scanning mutagenesis and a few other residues in close contact with the drug are shown in stick mode. Except for V659 and N658 all "high impact" residues from the scanning mutagenesis are in close contact with ICA. In both the open and closed states of the channel ICA resides in a hydrophobic pocket formed by L622, F619, F557, Y652 and F656. ICA interacts with F619, F557 and Y652 via $\pi - \pi$ stacking and stabilizes the Y652 side chain in the down conformation (towards the cytoplasmic side of channel) in agreement with previous MD simulations (Zachariae et al., 2009). In addition, hydrogen bonds are (frequently) predicted between ICA and the backbone of L622, the side chain and/or backbone of S624, T623 and S649 (Supplemental Figs. 4A and B).

The predicted binding mode of ICA is altered by the mutations that eliminated the activator effects of ICA (Supplemental Figs. 4 and 5). Atomistic molecular dynamics simulations revealed conformational changes in hERG1. For example, the F557L mutation induced side chain rotations of several residues (L646, F619, L622, T623) that reduce the size of the lipophilic pocket. In F557L and L622C mutant channels, ICA bound to the outside of the pore module. A653M allosterically reorients the side chains of F619, L622 and F557, removing the lipophilic pocket. In addition, in A653M channels, hydrogen bonds to Y652 and S649 (in S6) and S624 and T623 (selectivity filter) are frequently predicted by GOLD, and in contrast to WT channels the Y652 side chain frequently adopts an up-conformation. The Chemscore scoring function was used to estimate free energies of binding (Gold.Chemscore.DG) of ICA and were averaged over the 10 best docking poses for WT and mutant channels. $\triangle$G in kJ/mol were -40.9 and -40.54 for WT channels in the closed and open states, respectively and were reduced in the closed state of

Molecular Pharmacology Fast Forward. Published on July 8, 2011 as DOI: 10.1124/mol.111.073809
This article has not been copyedited and formatted. The final version may differ from this version.

the mutant channels as follows: -32.97 (F557L), -36.09 (L622C), -37.69 (Y652A) and -38.21 (A653M).

A single residue in S5 of hERG1 determines if ICA is an activator or inhibitor. We next determined the effects of ICA on a mutant hERG1 channel that does not inactivate. Combined mutation of two residues (G628C/S631C) located near or within the selectivity filter of hERG1 completely removes channel inactivation and reduces K^+ selectivity (Smith et al., 1996). Currents conducted by G628C/S631C hERG1 channels were not augmented by ICA; instead, 30 μM of the drug decreased currents by 40% (Fig. 6A, B). This reduction of current could result from drug binding to the central cavity receptor described for potent hERG1 blockers (Mitcheson et al., 2000). An important component of the blocker binding site is Y652 and mutations of this residue can greatly attenuate drug-induced block of WT channels. However, introduction of the Y652A mutation did not alter the response of G628C/S631C hERG1 channels to ICA (Fig. 6C), suggesting that current reduction is not caused by binding of ICA to the central cavity. Moreover, introduction of the F557L mutation (that prevents activator effects on WT channels) eliminated the response of G628C/S631C hERG1 channels to ICA (Fig. 6D). Together these findings suggest that ICA exerts its agonist and antagonist effects by binding to a single or overlapping receptor.

Discussion

Activation of hERG1 channels by ICA is state-independent and mediated by a pronounced positive shift in the voltage dependence of P-type inactivation (Gerlach et al., 2010). P-type inactivation is caused by very subtle changes in the dynamic structure of the selectivity filter (Cuello et al., 2010b). Mutation of residues located within or near the PH/SF that impaired inactivation (S620T, S631A) caused reduced sensitivity to the drug. Inhibition of a mutant channel (G628C/S631C hERG1) with inactivation removed (Smith et al., 1996) revealed that ICA also has intrinsic antagonist activity. F557 (S5) and L622 (PH) are considered to be the most

Molecular Pharmacology Fast Forward. Published on July 8, 2011 as DOI: 10.1124/mol.111.073809
This article has not been copyedited and formatted. The final version may differ from this version.

critical determinants of the binding site since single mutations of either residue prevented drug-induced changes in current magnitude and kinetics.

Voltage-gated channels can be considered analogous to intrinsically active receptors that are modulated by voltage. Viewed in this manner, ICA can behave as either an agonist or an inverse agonist of hERG1 channels. The drug is an agonist (i.e., activator) when bound to WT hERG1 channels, and an inverse agonist (i.e., inhibitor) when bound to A653M or G628C/S631C hERG1 channels. Strictly speaking, the term inverse agonist would apply only if ICA bound to the same site to mediate both activator and inhibitory effects. Inhibition of non-inactivating mutant hERG1 channels could simply result from pore block, mediated by binding of ICA to the central cavity as described for a plethora of hERG1 blockers (Mitcheson et al., 2000; Sanguinetti and Mitcheson, 2005) and distinct from the proposed activator site. Alternatively, both activation and inhibition of channel activity by ICA could arise from its binding to a single site as proposed for dihydropyridines that can either activate or inhibit L-type Ca^{2+} channels (Hockerman et al., 1997). For several reasons, we favor the hypothesis that ICA binds to a single site in both WT or mutant channels, and that current inhibition results from stabilization of channels in a closed (or inactivated) state rather than pore blockage per se. First, the putative activator site described for WT channels should remain intact in G628C/S631C hERG1 channels - lack of drug effect on F557L/G628C/S631C hERG1 channels supports this view. Second, if ICA bound to the well characterized central cavity site (Mitcheson et al., 2000), mutation of Y652 or F656 in hERG1 would be expected to cause an enhanced activator response rather than the observed diminished response. The side-chains of these aromatic residues are the most important molecular determinants of many hERG1 blockers (Sanguinetti and Mitcheson, 2005). Mutation of F656 to Thr enhanced the activator effect of NS1643 compared to WT channels (Casis et al., 2006), consistent with two binding sites for this compound – one that mediates activation and another (in the central cavity) that mediates pore block. In contrast, F656T channels were less sensitive to ICA. Third, a conserved Phe in S5 was a key determinant of both activator and inhibitory effects

Molecular Pharmacology Fast Forward. Published on July 8, 2011 as DOI: 10.1124/mol.111.073809
This article has not been copyedited and formatted. The final version may differ from this version.

of ICA in hERG1 channels. Mutation of F557 to Leu in hERG1 (F557L) eliminated all effects of the drug. Finally, A653M hERG1 channels exhibit normal inactivation, but currents were inhibited and deactivation was accelerated by the drug. Modeling suggests that the A653M mutation reverses the orientation of the side-chain of Y652 (from a down to an up configuration); perhaps this interferes with the coupling between drug binding and altered inactivation gating. Whatever the underlying mechanisms, A653M in hERG1 reveals an intrinsic antagonist activity of ICA that is normally masked by its dominant activator effect. A similar switch from agonist to antagonist activity was reported for (-)BayK 8644 after mutation of two adjacent residues (Y1485, M1486) in Domain IV S6 of the α_{1c} L-type Ca channel (Schuster et al., 1996). It is noteworthy that the topology of the putative ICA binding site, a hydrophobic pocket located between two adjacent subunits of the pore module, is similar to the proposed dihydropyridine binding site in L-type calcium channels (Cosconati et al., 2007; Tikhonov and Zhorov, 2009) and the binding site for brevetoxins and ciguatoxin (neurotoxin receptor site 5) in voltage-gated sodium channels (Catterall et al., 2007). All of these lipophilic compounds alter channel gating and are proposed to gain direct access to the pore module via the lipid membrane.

Mutation of Y652 to Ala prevents the attenuation of inactivation normally caused by RPR260243 (Perry et al., 2007). However, deactivation of Y652A hERG1 channels is markedly slowed by RPR260243 (Perry et al., 2007), indicating that the mutation does not prevent drug binding. Y652A channels are also resistant to the normally pronounced effect of ICA on inactivation. However, opposite to the effects on WT channels, deactivation of Y652A channels was accelerated by ICA. The ability of both ICA and RPR260243 to affect deactivation, but not inactivation of Y652A channels suggests that Y652 residues are required for coupling drug binding to suppression of channel inactivation. Modeling suggests that Y652 directly interacts with ICA, but not with RPR (Perry et al., 2007). Based on sequence alignments of S6 segments, Y652 is equivalent to F103 of KcsA and I470 of Shaker K^+ channels. Mutation of F103 (KcSA channel) or I470 (Shaker channel) drastically suppresses C-type inactivation, and Cuello et al

Molecular Pharmacology Fast Forward. Published on July 8, 2011 as DOI: 10.1124/mol.111.073809
This article has not been copyedited and formatted. The final version may differ from this version.

(Cuello et al., 2010a) have proposed that these key residues in S6 allosterically couple the cytosolic gate with the extracellular gate (SF), so-called bidirectional coupling. In contrast, mutations of Y652 in hERG1 do not appreciably alter inactivation gating (Fernandez et al., 2004). The mechanism responsible for disrupted coupling between drug binding and altered inactivation of Y652A hERG1 channels requires further study.

In summary, ICA binds to a hydrophobic pocket located between two adjacent hERG1 channel subunits resulting in a subtle change in configuration of the selectivity filter that disrupts inactivation gating. Binding of ICA to the same or overlapping site mediates inhibition of mutant A653M and G628C/S631C hERG1 channels.

Molecular Pharmacology Fast Forward. Published on July 8, 2011 as DOI: 10.1124/mol.111.073809
This article has not been copyedited and formatted. The final version may differ from this version.

Acknowledgements:

We thank Jennifer Abbruzzese for measurement of gating currents, Tobias Linder and Kirsten Knape for help with modeling figures, and Kam Hoe Ng for isolation and injection of oocytes.

Molecular Pharmacology Fast Forward. Published on July 8, 2011 as DOI: 10.1124/mol.111.073809
This article has not been copyedited and formatted. The final version may differ from this version.

Authorship Contributions:

Participated in research design: Garg, Sanguinetti.

Conducted experiments: Garg, Sanguinetti.

Performed data analysis: Garg, Sachse, Sanguinetti, Stary-Weinzinger.

Wrote or contributed to the writing of the manuscript: Garg, Sanguinetti, Stary-Weinzinger.

Molecular Pharmacology Fast Forward. Published on July 8, 2011 as DOI: 10.1124/mol.111.073809
This article has not been copyedited and formatted. The final version may differ from this version.

REFERENCES

Berger O, Edholm O and Jahnig F (1997) Molecular dynamics simulations of a fluid bilayer of dipalmitoylphosphatidylcholine at full hydration, constant pressure, and constant temperature. *Biophys J* **72**:2002-2013.

Bezanilla F and Stefani E (1998) Gating currents. *Methods Enzymol* **293**:331-352.

Brugada R, Hong K, Dumaine R, Cordeiro J, Gaita F, Borggrefe M, Menendez TM, Brugada J, Pollevick GD, Wolpert C, Burashnikov E, Matsuo K, Wu YS, Guerchicoff A, Bianchi F, Giustetto C, Schimpf R, Brugada P and Antzelevitch C (2004) Sudden death associated with short-QT syndrome linked to mutations in HERG. *Circulation* **109**:30-35.

Casis O, Olesen SP and Sanguinetti MC (2006) Mechanism of action of a novel human ether-a-go-go-related gene channel activator. *Mol Pharmacol* **69**:658-665.

Catterall WA, Cestele S, Yarov-Yarovoy V, Yu FH, Konoki K and Scheuer T (2007) Voltage-gated ion channels and gating modifier toxins. *Toxicon* **49**:124-141.

Cosconati S, Marinelli L, Lavecchia A and Novellino E (2007) Characterizing the 1,4-dihydropyridines binding interactions in the L-type Ca^{2+} channel: model construction and docking calculations. *J Med Chem* **50**:1504-1513.

Cuello LG, Jogini V, Cortes DM, Pan AC, Gagnon DG, Dalmas O, Cordero-Morales JF, Chakrapani S, Roux B and Perozo E (2010a) Structural basis for the coupling between activation and inactivation gates in K^+ channels. *Nature* **466**:272-275.

Cuello LG, Jogini V, Cortes DM and Perozo E (2010b) Structural mechanism of C-type inactivation in K^+ channels. *Nature* **466**:203-208.

Curran ME, Splawski I, Timothy KW, Vincent GM, Green ED and Keating MT (1995) A molecular basis for cardiac arrhythmia: *HERG* mutations cause long QT syndrome. *Cell* **80**:795-803.

Darden T, York D and Pedersen L (1993) Particle mesh Ewald: An N [center-dot] log(N) method for Ewald sums in large systems. *J Chem Physics* **98**:10089-10092.

Fernandez D, Ghanta A, Kauffman GW and Sanguinetti MC (2004) Physicochemical features of the hERG channel drug binding site. *J Biol Chem* **279**:10120-10127.

Ficker E, Jarolimek W, Kiehn J, Baumann A and Brown AM (1998) Molecular determinants of dofetilide block of HERG K^+ channels. *Circ Res* **82**(3):386-395.

Frisch MJ, Trucks GW, Schlegel HB, Scuseria GE, Robb MA, Cheeseman JR and Scalmani G (2009) *Gaussian 09, Revision A.1* Gaussian, Inc., Wallingford.

Gerlach AC, Stoehr SJ and Castle NA (2010) Pharmacological removal of human ether-a-go-go-related gene potassium channel inactivation by 3-nitro-N-(4-phenoxyphenyl) benzamide (ICA-105574). *Mol Pharmacol* **77**:58-68.

Goldenberg I and Moss AJ (2008) Long QT syndrome. *J Am Coll Cardiol* **51**:2291-2300.

Goldin AL (1991) Expression of ion channels by injection of mRNA into Xenopus oocytes. *Methods Cell Biol* **36**:487-509.

Hamill OP, Marty A, Neher E, Sakmann B and Sigworth FJ (1981) Improved patch-clamp techniques for high-resolution current recording from cells and cell-free membrane patches. *Pflugers Arch* **391**:85-100.

Hansen RS, Diness TG, Christ T, Demnitz J, Ravens U, Olesen SP and Grunnet M (2006) Activation of human ether-a-go-go-related gene potassium channels by the diphenylurea 1,3-bis-(2-hydroxy-5-trifluoromethyl-phenyl)-urea (NS1643). *Mol Pharmacol* **69**:266-277.

Hess B, Bekker H, Berendsen HJC and Fraaije JGEM (1997) LINCS: A linear constraint solver for molecular simulations. *J Computational Chem* **18**:1463-1472.

Hess B, Kutzner C, van der Spoel D and Lindahl E (2008) GROMACS 4: Algorithms for highly efficient, load-balanced, and scalable molecular simulation. *J Chem Theory Comput* **4**:435–447.

Hockerman GH, Peterson BZ, Johnson BD and Catterall WA (1997) Molecular determinants of drug binding and action on L-type calcium channels. *Annu Rev Pharmacol Toxicol* **37**:361-396.

Jones G, Willett P and Glen RC (1995) Molecular recognition of receptor sites using a genetic algorithm with a description of desolvation. *J Mol Biol* **245**:43-53.

Jorgensen WL, Chandrasekhar J, Madura JD, Impey RW and M.L. K (1983) Comparison of simple potential functions for simulating liquid water. *J Chem Physics* **79**:926-935.

Jorgensen WL, Maxwell DS and Tirado-Rives J (1996) Development and Testing of the OPLS All-Atom Force Field on Conformational Energetics and Properties of Organic Liquids. *J Am Chem Soc* **118**:11225-11236.

Kang J, Chen XL, Wang H, Ji J, Cheng H, Incardona J, Reynolds W, Viviani F, Tabart M and Rampe D (2005) Discovery of a small molecule activator of the Human Ether-a-go-go-Related Gene (HERG) cardiac K^+ channel. *Mol Pharmacol* **67**:827-836.

Mitcheson JS, Chen J, Lin M, Culberson C and Sanguinetti MC (2000) A structural basis for drug-induced long QT syndrome. *Proc Natl Acad Sci USA* **97**:12329-12333.

Nose S (1984) A unified formulation of the constant temperature molecular dynamics methods. *The Journal of Chemical Physics* **81**:511-519.

Parrinello M and Rahman A (1981) Polymorphic transitions in single crystals: A new molecular dynamics method. *J Applied Physics* **52**:7182-7190.

Perry M, Sachse FB, Abbruzzese J and Sanguinetti MC (2009) PD-118057 contacts the pore helix of hERG1 channels to attenuate inactivation and enhance K^+ conductance. *Proc Natl Acad Sci USA* **106**:20075-20080.

Perry M, Sachse FB and Sanguinetti MC (2007) Structural basis of action for a human ether-a-go-go-related gene 1 potassium channel activator. *Proc Natl Acad Sci USA* **104**:13827–13832.

Piper DR, Varghese A, Sanguinetti MC and Tristani-Firouzi M (2003) Gating currents associated with intramembrane charge displacement in HERG potassium channels. *Proc Natl Acad Sci USA* **100**:10534-10539.

Sanguinetti MC, Jiang C, Curran ME and Keating MT (1995) A mechanistic link between an inherited and an acquired cardiac arrhythmia: *HERG* encodes the I_{Kr} potassium channel. *Cell* **81**:299-307.

Sanguinetti MC and Mitcheson JS (2005) Predicting drug-hERG channel interactions that cause acquired long QT syndrome. *Trends Pharmacol Sci* **26**:119-124.

Sanguinetti MC and Tristani-Firouzi M (2006) hERG potassium channels and cardiac arrhythmia. *Nature* **440**:463-469.

Schonherr R and Heinemann SH (1996) Molecular determinants for activation and inactivation of HERG, a human inward rectifier potassium channel. *J Physiol* **493**:635-642.

Schreibmayer W, Lester HA and Dascal N (1994) Voltage clamping of Xenopus laevis oocytes utilizing agarose-cushion electrodes. *Pflugers Arch* **426**:453-458.

Schuster A, Lacinova L, Klugbauer N, Ito H, Birnbaumer L and Hofmann F (1996) The IVS6 segment of the L-type calcium channel is critical for the action of dihydropyridines and phenylalkylamines. *EMBO J* **15**:2365-2370.

Smith PL, Baukrowitz T and Yellen G (1996) The inward rectification mechanism of the HERG cardiac potassium channel. *Nature* **379**:833-836.

Stary A, Wacker SJ, Boukharta L, Zachariae U, Karimi-Nejad Y, Aqvist J, Vriend G and de Groot BL (2010) Toward a consensus model of the HERG potassium channel. *ChemMedChem* **5**:455-467.

Stefani E and Bezanilla F (1998) Cut-Open Oocyte Voltage-Clamp Technique, in *Methods in Enzymology* (Conn PN ed) pp 300-318, Academic Press, San Diego.

Stuhmer W (1992) Electrophysiological recording from *Xenopus* oocytes. *Methods Enzymol* **207**:319-339.

Tikhonov DB and Zhorov BS (2009) Structural model for dihydropyridine binding to L-type calcium channels. *J Biol Chem* **284**:19006-19017.

Trudeau M, Warmke JW, Ganetzky B and Robertson GA (1995) HERG, A human inward rectifier in the voltage-gated potassium channel family. *Science* **269**:92-95.

Witchel HJ, Milnes JT, Mitcheson JS and Hancox JC (2002) Troubleshooting problems with in vitro screening of drugs for QT interval prolongation using HERG K^+ channels expressed in mammalian cell lines and *Xenopus* oocytes. *J Pharmacol Toxicol Methods* **48**(2):65-80.

Zachariae U, Giordanetto F and Leach AG (2009) Side chain flexibilities in the human ether-a-go-go related gene potassium channel (hERG) together with matched-pair binding studies suggest a new binding mode for channel blockers. *J Med Chem* **52**:4266-4276.

Zhou J, Augelli-Szafran CE, Bradley JA, Chen X, Koci BJ, Volberg WA, Sun Z and Cordes JS (2005) Novel potent human ether-a-go-go-related gene (hERG) potassium channel enhancers and their in vitro antiarrhythmic activity. *Mol Pharmacol* **68**:876-884.

Zou A, Curran ME, Keating MT and Sanguinetti MC (1997) Single HERG delayed rectifier K^+ channels in *Xenopus* oocytes. *Am J Physiol* **272**:H1309-H1314.

Molecular Pharmacology Fast Forward. Published on July 8, 2011 as DOI: 10.1124/mol.111.073809
This article has not been copyedited and formatted. The final version may differ from this version.

Footnotes:

This work was supported by National Institutes of Health/National Heart, Lung, and Blood Institute [Grant HL055236] to M.S., an American Heart Association (Western States Affiliate) postdoctoral fellowship to V.G., and The Austrian Science Fund [Grant P22395] to A. S.-W.

Reprint requests: M.C. Sanguinetti, Nora Eccles Harrison Cardiovascular Research & Training Institute, Department of Physiology, University of Utah, 95 South 2000 East, Salt Lake City, UT 84112; E-mail: sanguinetti@cvrti.utah.edu

Molecular Pharmacology Fast Forward. Published on July 8, 2011 as DOI: 10.1124/mol.111.073809
This article has not been copyedited and formatted. The final version may differ from this version.

Figure Legends

Fig. 1. Voltage-dependent activation of hERG1 current by ICA-105574 (ICA) in *Xenopus* oocytes. (A) ICA increases the magnitude of hERG1 current. Currents were elicited with 1-s pulses to test potentials applied in 10 mV increments from –80 to +50 mV. Tail currents (I_{tails}) were measured at –70 mV. Voltage protocol is shown above control current traces. (B) *I*-Vt relationships measured before (Control) and in presence of 10 and 30 μM ICA (*n* = 3-8). Currents were normalized relative to the peak outward control current at +20 mV. (C) Fold-increase in normalized peak outward current induced by 30 μM ICA plotted as a function of Vt (*n* = 8). (D*)* ICA binds to open/inactivated state of hERG1 channels. Upper panel shows voltage clamp protocol. Middle panel is corresponding current trace showing time of application of 10 μM ICA (arrow). After several minutes at +30 mV, the voltage was progressively stepped down from 0 to -80 mV in 20 mV increments. Lower panel is a plot of current magnitude at +30 mV before (control) and after 10 min in the presence of 10 μM ICA (*n* = 4). *(*E*)* Plot of peak I_{tail} versus Vt determined before and after 30 μM ICA in oocytes bathed in 104 mM $[K^+]_e$ solution. Currents were activated with 1-s pulses to a variable Vt and I_{tail} was measured at –140 mV. Peak I_{tail} magnitude was determined by fitting the current decay to a biexponential function and extrapolating the fit to the onset of membrane repolarization then normalized relative to the peak of control I_{tail} for each oocyte. Data were fitted with a Boltzmann function (smooth curves). For control, $V_{0.5}$ = –22 ± 0.5 mV, k = 8.8 ± 0.3 mV; for ICA, $V_{0.5}$ = –22.9 ± 0.3 mV, k = 9.3 ± 0.2 mV (*n* = 9). (F) Single channel *i*-Vt relationship determined for cell-attached patches from oocytes bathed in control or 30 μM ICA solution. Slope conductance determined by linear fit of data for the Vt range of –100 mV to –180 mV was 18.1 ± 0.39 pS (*n* = 10) in control patches, and 18.6 ± 0.28 pS (*n* = 10) in the presence of 30 μM ICA. (G). ICA does not alter the voltage dependence or maximal value of charge displacement ($Q_{OFF\text{-}max}$) associated with the OFF gating

Molecular Pharmacology Fast Forward. Published on July 8, 2011 as DOI: 10.1124/mol.111.073809
This article has not been copyedited and formatted. The final version may differ from this version.

current of hERG1 channels. Normalized $Q_{OFF\text{-}max}$ was plotted as a function of Vt and fitted with a Boltzmann function (smooth curves). For control, $V_{0.5}$ = –14.0 ± 0.6 mV, k = 14.1 ± 0.3 mV; for ICA, $V_{0.5}$ = –9.7 ± 0.1 mV, k = 14.7 ± 0.3 mV (*n* = 9). The slight shift in $V_{0.5}$ was also observed for vehicle (DMSO) control (see Supplemental Fig. 1).

Fig. 2. Mutant channels with impaired inactivation are less sensitive to ICA. (A) S620T hERG1 currents recorded before (Control) and after 30 μM ICA (left and middle panels). Currents were elicited as described in Fig. 1A. Right panel shows plots of mean *I*-Vt relationships determined before (■) and after 30 μM ICA (○). Currents (I_{test}) were measured at the end of 1-s test pulses and normalized relative to the peak outward value of control currents (*n* = 7). (B and C) Current traces (*Left and middle panels*) and *I*-Vt relationships (*Right panel*) for S631A (*n* = 4) and N558K (*n* = 3) hERG1 channels.

Fig. 3. Molecular determinants of hERG1 channel sensitivity to ICA. (A) Sequence of the S5 and pore helix-S6 domains of a hERG1 subunit. The S5, pore helix and S6 segments are underlined, and the scanned residues are indicated by bold text. (B) Bar graph summarizing fold-increase in hERG1 current magnitude at +20 mV induced by 30 μM ICA for WT (black bar) or channels containing single point mutations as indicated. 'High impact' residues (≥10-fold reduction in drug effect as compared to WT hERG1, $p<0.0005$) are indicated by checkered bars. Vehicle control (DMSO) had no effect. NE, no functional expression.

Fig. 4. Mutation of F557, L622, Y652 or A653 eliminates or reverses agonist activity of ICA on hERG1. (A) *Left and middle panels*: F557L hERG1 currents (elicited as described in Fig. 1*A*) recorded before (Control) and after 30 μM ICA. *Right panel*: *I*-Vt relationships for currents at the end of 1-s test pulse determined before (■) and after treatment of cells with 30 μM ICA (○).

Molecular Pharmacology Fast Forward. Published on July 8, 2011 as DOI: 10.1124/mol.111.073809
This article has not been copyedited and formatted. The final version may differ from this version.

Currents were normalized relative to peak outward value of control current. (B - D) Current traces (*Left and middle panels*) and *I*-Vt relationships (*Right panel*) for L622C (B), Y652A (C) and A653M (D) hERG1 channels.

Fig. 5. ICA docked to a KvAP- (open-state) and KcsA- (closed-state) based homology model of the hERG1 pore module. (A) Open-state pore module of the channel (ribbons) as viewed from the extracellular space. ICA is shown in space fill. (B) Close-up view of the putative drug-binding region to the open state channel. Residues designated as "high impact" based on scanning mutagenesis using low $[K^+]_e$ solution (F557, F619, L622, S624, Y652, A653, F656, V659, N658) or high $[K^+]_e$ solution (T623, M645) are labeled and are shown as stick models. Also labeled is one additional residue (L646) predicted to be in close contact with drug that exhibited a normal drug response when mutated to Ala. (C) ICA binding to the closed-state pore module of the channel as viewed from the extracellular space. (D) Close-up view of the putative drug-binding region with labeling the same as in panel B.

Fig. 6. Mutation of Phe to Leu in S5 eliminates the inhibitory effect of ICA in a non-inactivating mutant hERG1 channel. (A) ICA inhibits non-inactivating G628C/S631C (GC/SC) hERG1 mutant channels. Currents were elicited as described in Fig. 1*A* and were recorded before (control) and after 10 min of 30 μM ICA. *(*B*) I*-Vt relationships for currents measured at the end of 1-s test pulses before (■) and after treatment of cells with 30 μM ICA (○). Currents were normalized relative to control current at +60 mV (n = 6). (C) Y652A/G628C/S631C hERG1 channels are also blocked by 30 μM ICA (○) (n = 8). (D) F557L/G628C/S631C hERG1 channels are insensitive to 30 μM ICA (○) *(*n = 12).

Figure 1

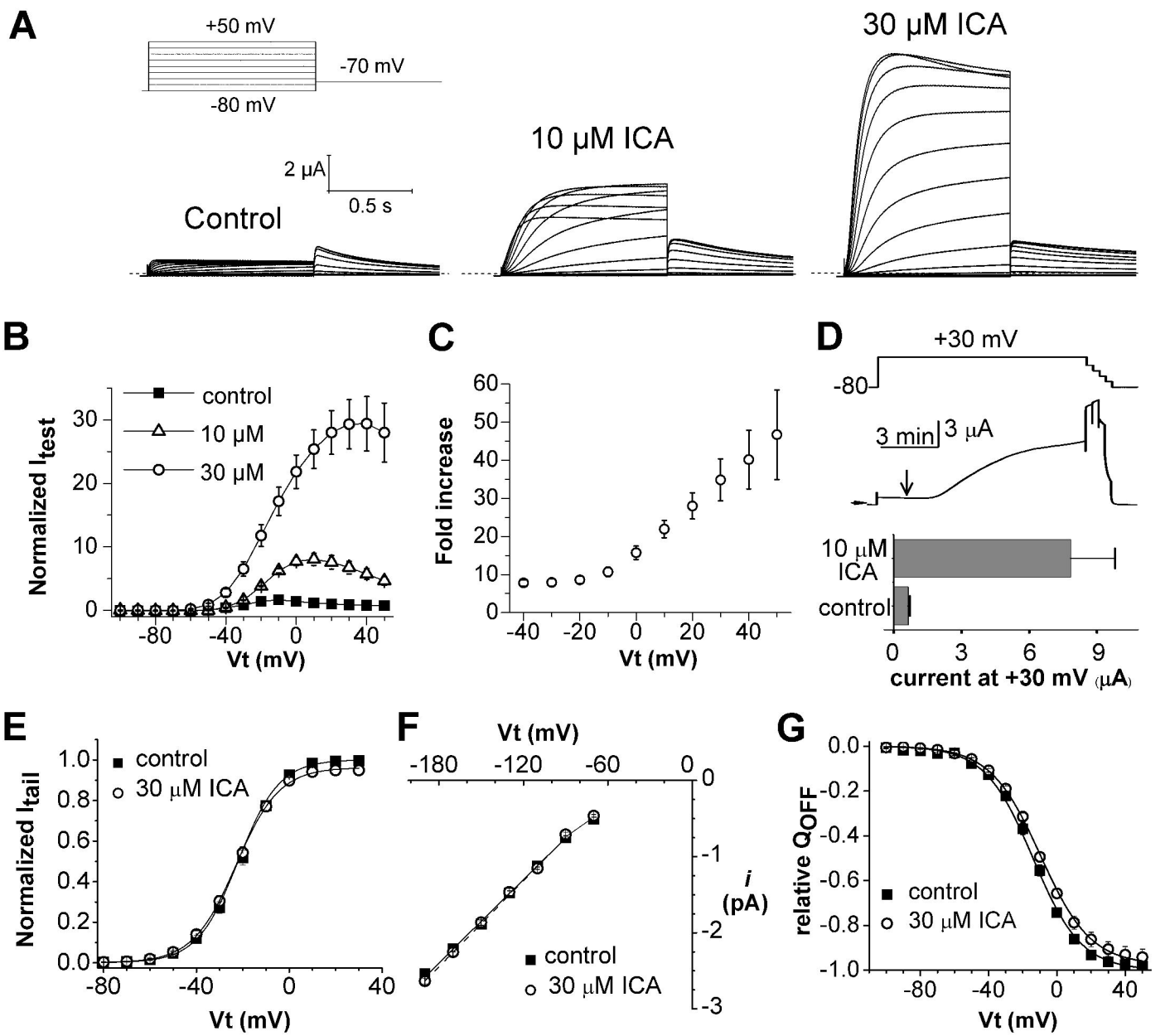
A
+50 mV
-70 mV
-80 mV
2 μA
0.5 s
Control
10 μM ICA
30 μM ICA
B
control
10 μM
30 μM
Normalized I_{test}
Vt (mV)
C
Fold increase
Vt (mV)
D
+30 mV
-80
3 min
3 μA
10 μM ICA
control
current at +30 mV (μA)
E
control
30 μM ICA
Normalized I_{tail}
Vt (mV)
F
Vt (mV)
control
30 μM ICA
i (pA)
G
relative Q_{OFF}
control
30 μM ICA
Vt (mV)

Figure 2

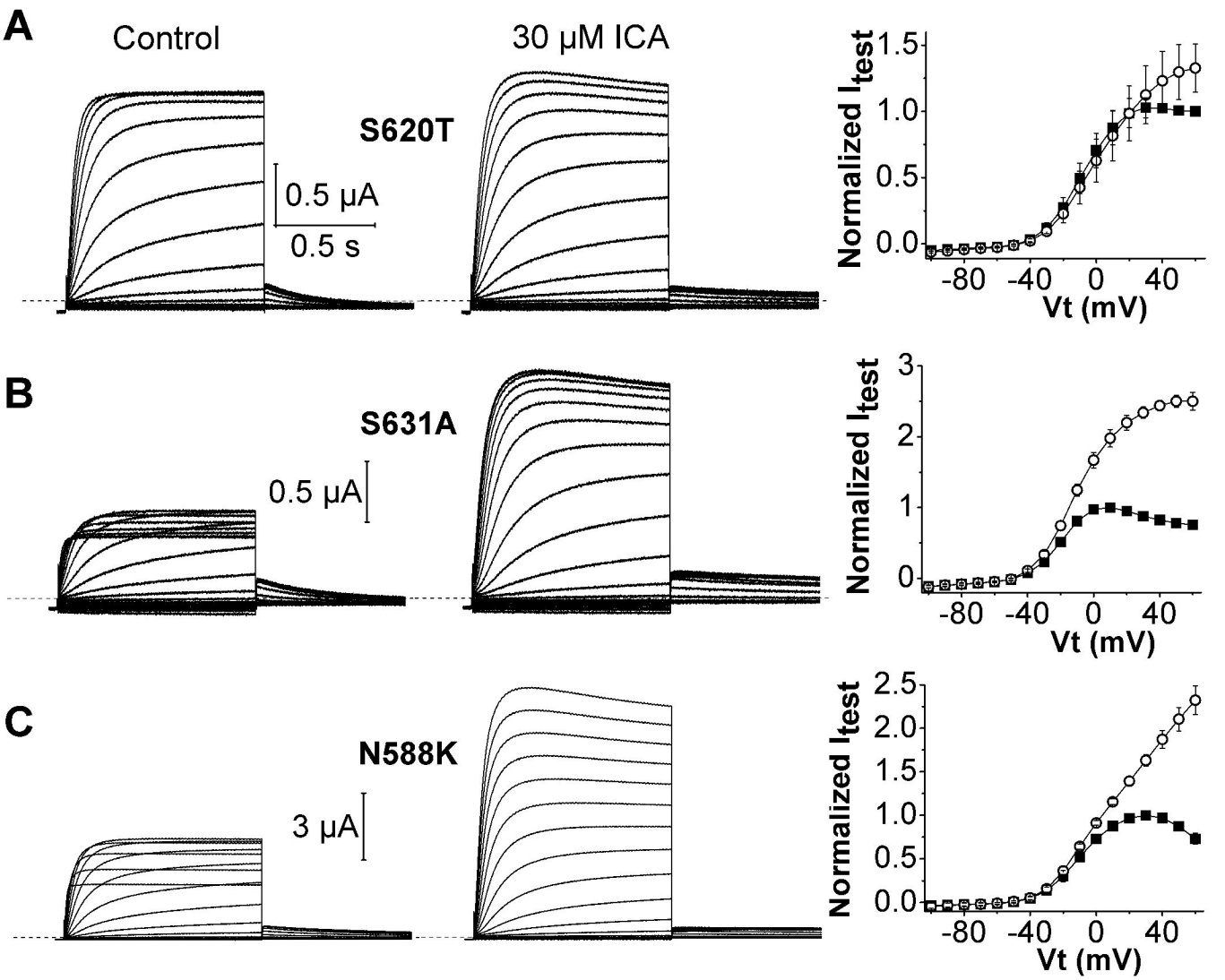
A
Control
30 μM ICA
S620T
0.5 μA
0.5 s
Normalized I test
1.5
1.0
0.5
0.0
-80 -40 0 40
Vt (mV)
B
S631A
0.5 μA
Normalized I test
3
2
1
0
-80 -40 0 40
Vt (mV)
C
N588K
3 μA
Normalized I test
2.5
2.0
1.5
1.0
0.5
0.0
-80 -40 0 40
Vt (mV)

Figure 3

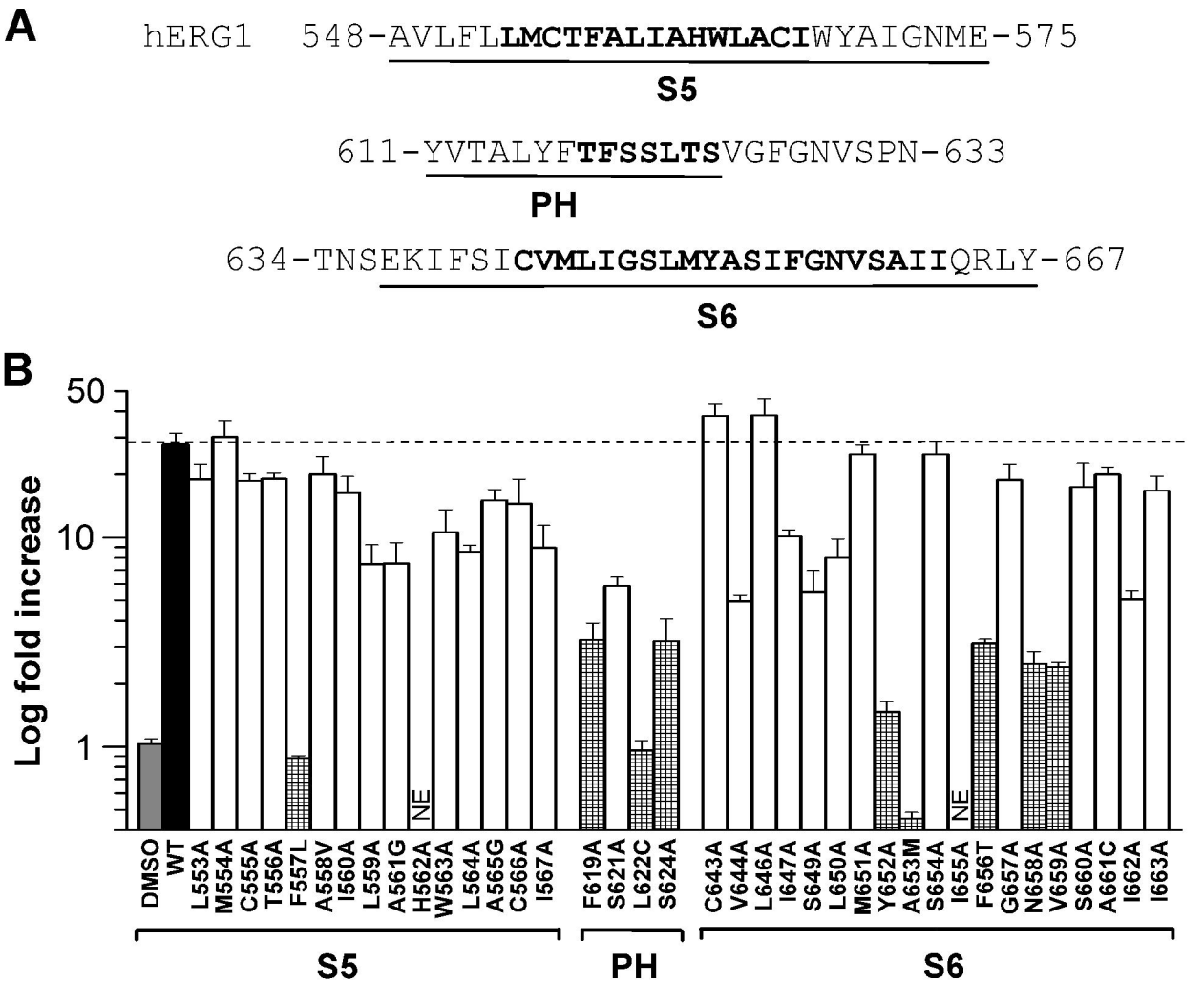
A
hERG1 548-AVLFLLMCTFALIAHWLACIWYAIGNME-575
S5
611-YVTALYFTFSSLTSVGFGNVSPN-633
PH
634-TNSEKIFSICVMLIGSLMYASIFGNVSAIIQRLY-667
S6
B
Log fold increase
50
10
1
NE
NE
DMSO
WT
L553A
M554A
C555A
T556A
F557L
A558V
I560A
L559A
A561G
H562A
W563A
L564A
A565G
C566A
I567A
F619A
S621A
L622C
S624A
C643A
V644A
L646A
I647A
S649A
L650A
M651A
Y652A
A653M
S654A
I655A
F656T
G657A
N658A
V659A
S660A
A661C
I662A
I663A
S5
PH
S6

Figure 4

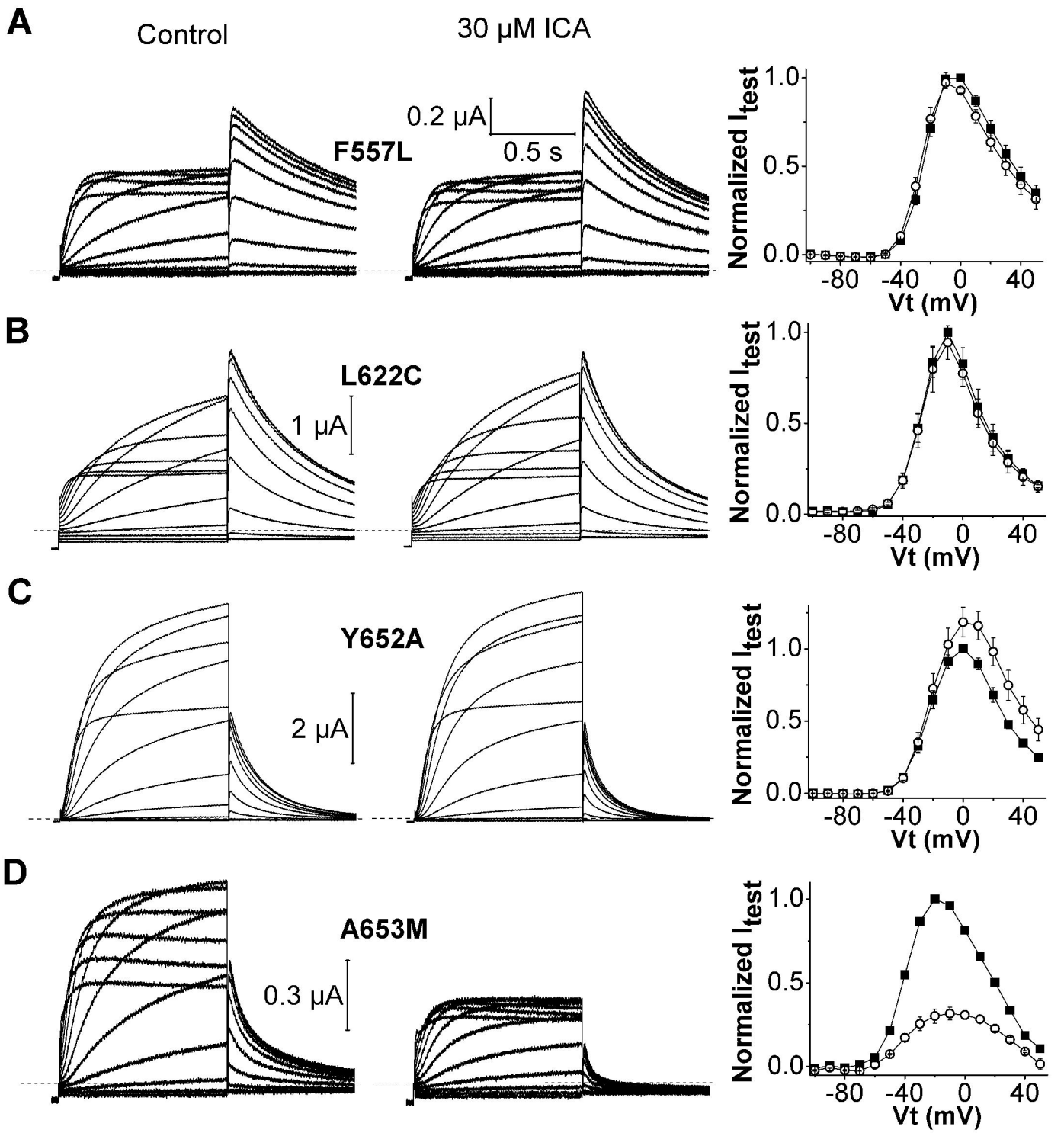
A
Control
30 μM ICA
0.2 μA
0.5 s
F557L
Normalized I test
1.0
0.5
0.0
-80
-40
0
40
Vt (mV)
B
L622C
1 μA
C
Y652A
2 μA
D
A653M
0.3 μA

Figure 5

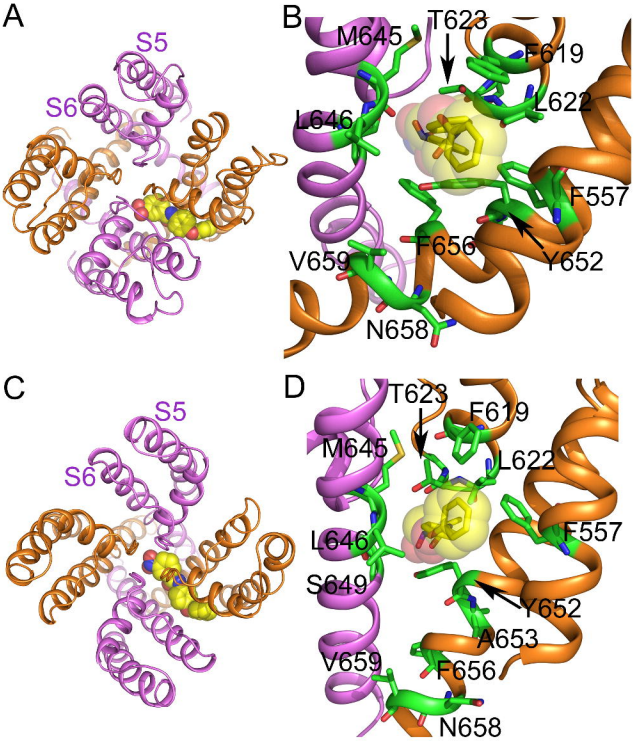
A
S5
S6
B
T623
M645
F619
L622
L646
F557
F656
Y652
V659
N658
C
S5
S6
D
T623
F619
M645
L622
F557
L646
S649
Y652
A653
V659
F656
N658

Figure 6

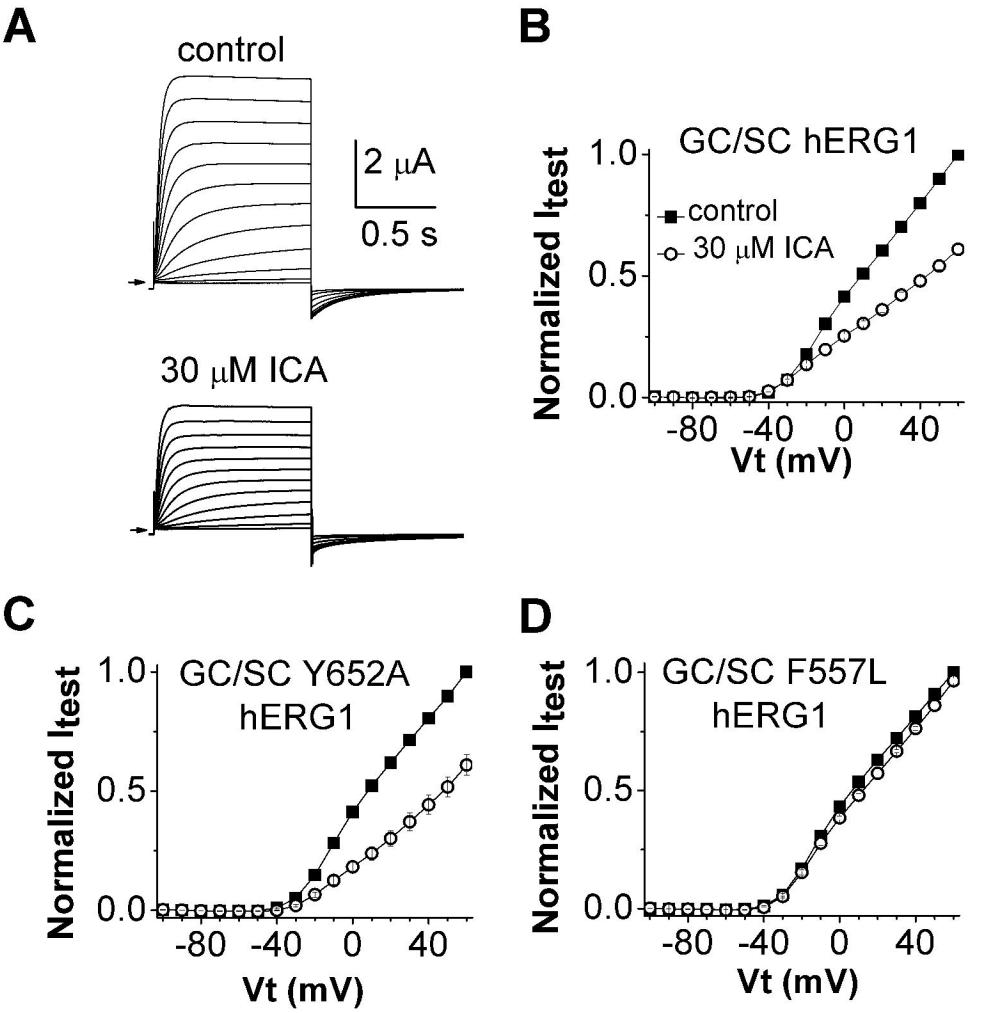
A
control
2 μA
0.5 s
30 μM ICA
B
GC/SC hERG1
control
30 μM ICA
Normalized Itest
1.0
0.5
0.0
-80 -40 0 40
Vt (mV)
C
GC/SC Y652A hERG1
Normalized Itest
1.0
0.5
0.0
-80 -40 0 40
Vt (mV)
D
GC/SC F557L hERG1
Normalized Itest
1.0
0.5
0.0
-80 -40 0 40
Vt (mV)